Cenozoic Volcanism of the La Bajada Constriction Area, New Mexico

By Ren A. Thompson, David A. Sawyer, Mark R. Hudson, V.J.S. Grauch, and W.C. McIntosh

Chapter C of
The Cerrillos Uplift, the La Bajada Constriction, and Hydrogeologic Framework of the Santo Domingo Basin, Rio Grande Rift, New Mexico
Edited by Scott A. Minor

Professional Paper 1720–C

U.S. Department of the Interior
U.S. Geological Survey

Contents

Figures

Tables

Cenozoic Volcanism of the La Bajada Constriction Area, New Mexico

By Ren A. Thompson, David A. Sawyer, Mark R. Hudson, V.J.S. Grauch, and W.C. McIntosh

Abstract

Late Tertiary to Quaternary volcanic rocks of the La Bajada constriction region, situated along the Rio Grande rift in northern New Mexico, consist of pre-rift and rift-related volcanic rocks of four discrete volcanic fields. These volcanic rocks include (1) a deeply dissected and incomplete section of pre-rift mafic- to intermediate-composition volcanic and volcaniclastic deposits exposed in the Cieneguilla area southeast of the La Bajada constriction; (2) intermediate- to silicic-composition pre-caldera and caldera-related rocks of the Jemez volcanic field west of the constriction; (3) basaltic volcanic rocks of the Santa Ana Mesa volcanic field in the center of the Santo Domingo basin; and (4) basaltic to intermediate-composition volcanic rocks of the Cerros del Rio volcanic field that overlap the eastern part of the constriction. All four of these volcanic fields are described in this chapter; and a primary focus is on the Cerros del Rio volcanic field because it bears most profoundly on the hydrogeologic framework and tectonic evolution of the La Bajada constriction.

The Plio-Pleistocene Cerros del Rio field is one of the largest (>700 km2) basaltic volcanic fields in the Rio Grande rift and preserves a record of the late-stage, volcano-tectonic evolution of the northeastern Santo Domingo and southwestern Española rift basins. Integrated geologic map, paleomagnetic, and aeromagnetic data were used to establish aerial distributions and stratigraphic relations of major eruptive units within the field. $^{40}Ar/^{39}Ar$ age determinations were used to establish timing of major eruptive episodes and, in conjunction with stratigraphic data, to provide temporal constraints on displacement of exposed or inferred faults within the volcanic field. Mostly flat-lying lava flows and pyroclastic deposits of the Cerro del Rio field erupted from multiple basaltic to dacitic volcanoes in three main phases. First-phase eruptions formed large volcanoes with constructive topography, such as Montoso Peak and Cerro Colorado, between 2.8 and 2.6 Ma during the normal-polarity Gauss magnetic chron and are associated with positive aeromagnetic anomalies. Second-phase eruptions issued from numerous smaller-volume vents; erupted lava flows commonly filled topographic lows between the older, larger volcanoes. These lavas were erupted between 2.5 and 2.2 Ma during the reversed-polarity Matuyama magnetic chron and, where sufficiently thick, are associated with negative aeromagnetic anomalies. A final 1.5- to 1.1-Ma eruptive phase is represented by the 1.46-Ma basaltic andesite of Cochiti Cone and smaller volume, younger volcanic centers in the western third of the Cerro del Rio field.

A series of northerly striking faults traversing the western part of the Cerro del Rio volcanic field down-dropped lava flows of the first- and second-phase eruptions into the actively subsiding northeastern margin of the Santo Domingo basin. Ancient down-to-west scarps along the Cochiti Cone fault and the La Bajada fault zone are locally mantled by volcanic deposits from Cochiti Cone, and similar buried faults likely controlled the emplacement of Cochiti Cone feeder dikes and edifice conduits. Older faults inferred from topographic lineaments are subparallel to these young faults and cut some second-stage volcanic centers. Younger second-stage centers form isolated and aligned zones of volcanic vents on strike with these inferred faults. Feeder dikes for these localized eruptive centers may have been emplaced along northerly striking fault zones within underlying basin-fill sediments of the Santa Fe Group.

Introduction

Studies by the U.S. Geological Survey were begun in 1996 to improve understanding of the geologic framework of the Albuquerque composite basin and adjoining areas, in order that more accurate hydrogeologic parameters could be applied to new hydrologic models. The ultimate goal of this multidisciplinary effort has been to better quantify estimates of future water supplies for northern New Mexico's growing urban centers, which largely subsist on aquifers in the Rio Grande rift basin (Bartolino and Cole, 2002). From preexisting hydrologic models it became evident that hydrogeologic uncertainties were large in the Santo Domingo Basin area, immediately up gradient from the greater Albuquerque metropolitan area, and particularly in the northeast part of the basin referred to as the La Bajada constriction (see chapter A, this volume, for a geologic definition of this feature as used in this report). Accordingly, a priority for new geologic and geophysical investigations was to better determine the hydrogeologic framework of the La Bajada constriction area. This chapter along with the other chapters of this report present the results of such investigations as recently conducted by the U.S. Geological Survey.

Overview of Regional Geology

Geologic Structure and Volcanism

The Rio Grande rift resulted from middle Cenozoic crustal extension in the southern Rocky Mountains. It is characterized by continental-scale rifting, subsidence of discrete basins, and uplift of rift margins. The continental extension was accompanied by lithospheric attenuation, asthenospheric upwelling, and intrarift magmatism. The ensuing volcanism spanned the range of terrestrial magma types and eruption modes, was largely episodic, and commonly reflected emplacement controlled by local structures superimposed on major crustal discontinuities.

In northern New Mexico, the Rio Grande rift is predominantly expressed by a series of north-trending, right-stepping en echelon grabens and half grabens that are structurally linked by northeast-trending accommodation zones. The most notable accommodation zone in the Jemez Mountains region is the Embudo fault zone (EB, fig. C1) that separates the east-dipping half-graben of the San Luis Basin from the west-dipping Española Basin. This accommodation zone coincides with the northeast-trending Jemez lineament (Mayo, 1958), a presumed Precambrian crustal shear zone or suture zone. Cenozoic volcanism marks the trend of the Jemez lineament (Luedke and Smith, 1978), the loci of which may reflect conduits for mantle-derived magmas that dominate post-Miocene volcanism (Baldridge, 1979a, Baldridge and others, 1984). Volcanism of the Jemez region is juxtaposed on the intersection of the Jemez lineament with the Rio Grande rift and is manifest in the long-lived, compositionally diverse Jemez field, which culminated in the spectacular caldera-forming eruption of the Bandelier Tuff rhyolites and shorter lived basaltic centers of the Cerros del Rio and Santa Ana Mesa volcanic fields (fig. C1). Eruption of synextensional mafic lavas is characteristic of magmatism in the Rio Grande rift (Lipman and Mehnert, 1979; Baldridge and others, 1980; Dungan and others, 1989; McMillan, 1998). The smaller mafic fields' proximity to the large-volume silicic field of the Jemez Mountains suggests that the lavas of the Cerros de Rio and Santa Ana Mesa volcanic fields reflect the large volumes of mafic magmas required to sustain the long-lived intermediate to silicic volcanism of the Jemez Mountains. However, it is likely that basaltic rift volcanism of the Cerros del Rio and Santa Ana Mesa fields is using structural weaknesses associated with late Pliocene extension as conduits for eruption of mafic magmas on the margins of the Jemez magmatic system.

A goal of this chapter is to better document the relation between volcanism and extensional faulting in the La Bajada constriction area. Many older structures that form the western boundary of the rift in the Jemez Mountains are largely buried beneath the latest plateau-forming outflow sheets of the Bandelier Tuff that erupted out of the Valles caldera. Likewise, pre-Pleistocene faults east of the Rio Grande are obscured by overlying upper Pliocene basaltic lavas of the Cerros del Rio volcanic field. The relation between major eruptive periods in the La Bajada constriction region and active extensional faulting is based in large part on new detailed geologic mapping and associated geochronologic studies (Smith and Kuhle, 1998a,b; Sawyer and others, 2002; R. Thompson, R. Shroba, and D. Dethier, unpub. data, 2005), fault studies (Minor and Hudson, 2006) (chapter E, this volume), and regional geophysical investigations (chapters D and F, this volume). The results of these efforts bear directly on interpretations of the subsurface configuration of the northeast part of the Santo Domingo Basin, the La Bajada constriction, the Cerrillos uplift, and the southern Española Basin. Consequently, a summary of the volcanic stratigraphy of the La Bajada constriction region (fig. C1), presented in this chapter, forms a basis for geochronologic constraints on the timing of late Cenozoic extension and faulting in the southwestern Española and northern Santo Domingo rift basins.

Figure C1 (following page). Location and general geology of the Jemez Mountains and adjacent basins of the Rio Grande rift. Double-headed arrows indicate approximate trend of the Jemez lineament. CDRVF, Cerros del Rio volcanic field; LBC, La Bajada constriction; SAMVF, Santa Ana Mesa volcanic field; TPVF, Taos Plateau volcanic field. Faults and fault zones: EB, Embudo; JZ, Jemez; LB, La Bajada; PJ, Pajarito. Rectangle shows location of figure C2, and inset map shows location of detailed map along Rio Grande rift in New Mexico.

Stratigraphic Framework

The stratigraphic framework of Cenozoic volcanic deposits in the La Bajada constriction region is complex, because it includes pre-rift and rift-related rocks from no fewer than four discrete volcanic fields. In the following section we describe (1) the pre-rift volcanic sequence and related sedimentary rocks in the southeastern part of the study area, (2) the regional stratigraphic relations of volcanic rocks of the Jemez and Santa Ana Mesa volcanic fields, and (3) rocks of the Cerros del Rio volcanic field. The Cerros del Rio field is the primary focus of this discussion owing to the juxtaposition of volcanic deposits of this field with major pre-rift and rift-related structures defining the La Bajada constriction and because of the temporal constraints on faulting provided by geochronologic and stratigraphic age control of major eruptive events of the Cerros del Rio.

The distribution of Cenozoic volcanic rocks and associated volcaniclastic sediments in the La Bajada constriction region is depicted in plate 2 and figure C2. Generalized volcanic stratigraphic sections, modified from plate 2, are presented in figure C3. Stratigraphic units are described based on historical or established nomenclature where feasible.

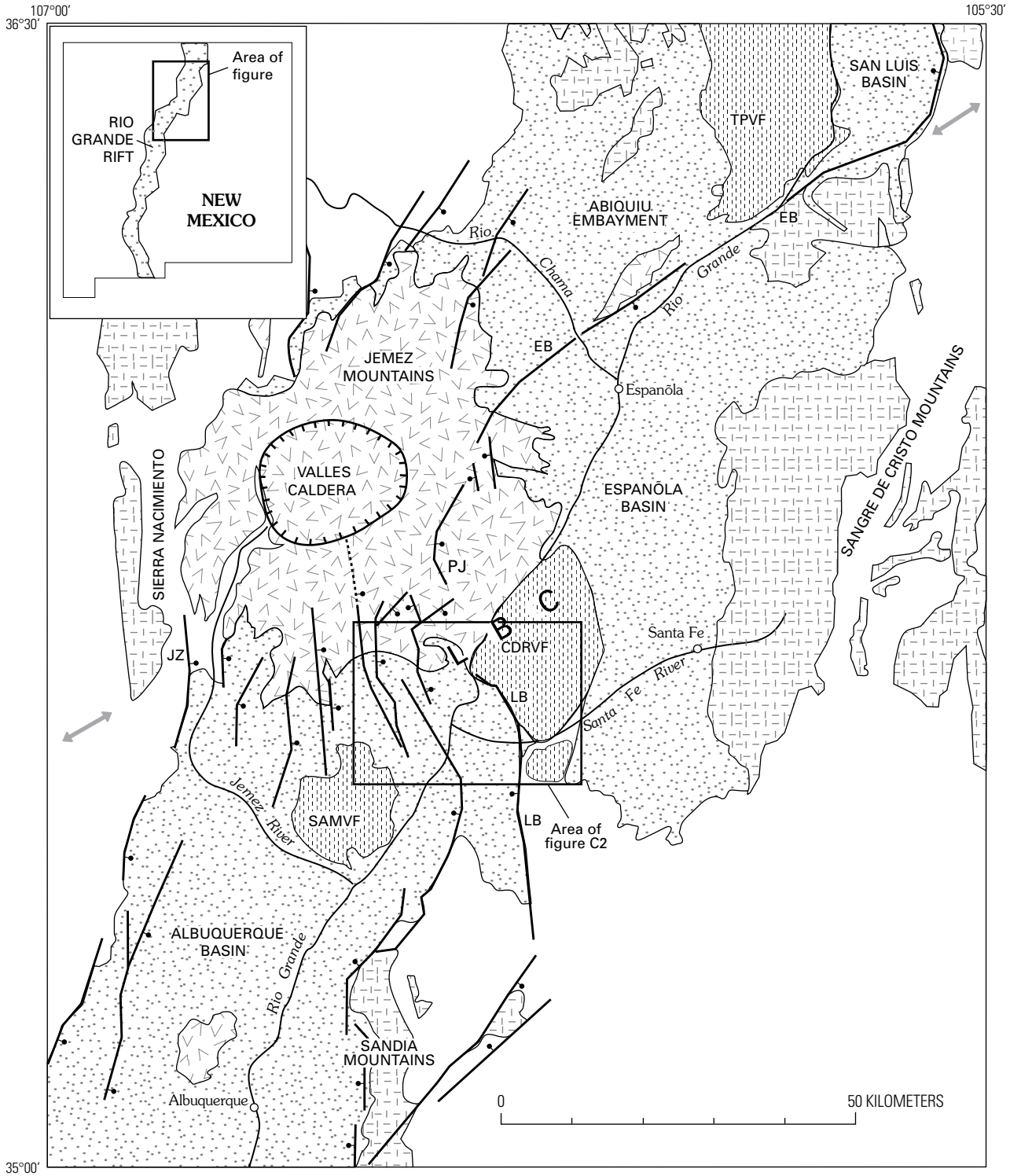

EXPLANATION

- Pleistocene–Pliocene basaltic volcanic fields
- Pleistocene–Miocene volcanic rocks
- Pleistocene–Oligocene basin-fill sediment
- Lower Oligocene–Paleozoic rocks
- Precambrian rocks
- **Major fault**—Bar and ball on downthrown block; dotted where concealed
- Boundary of caldera
- Trend of Jemez lineament

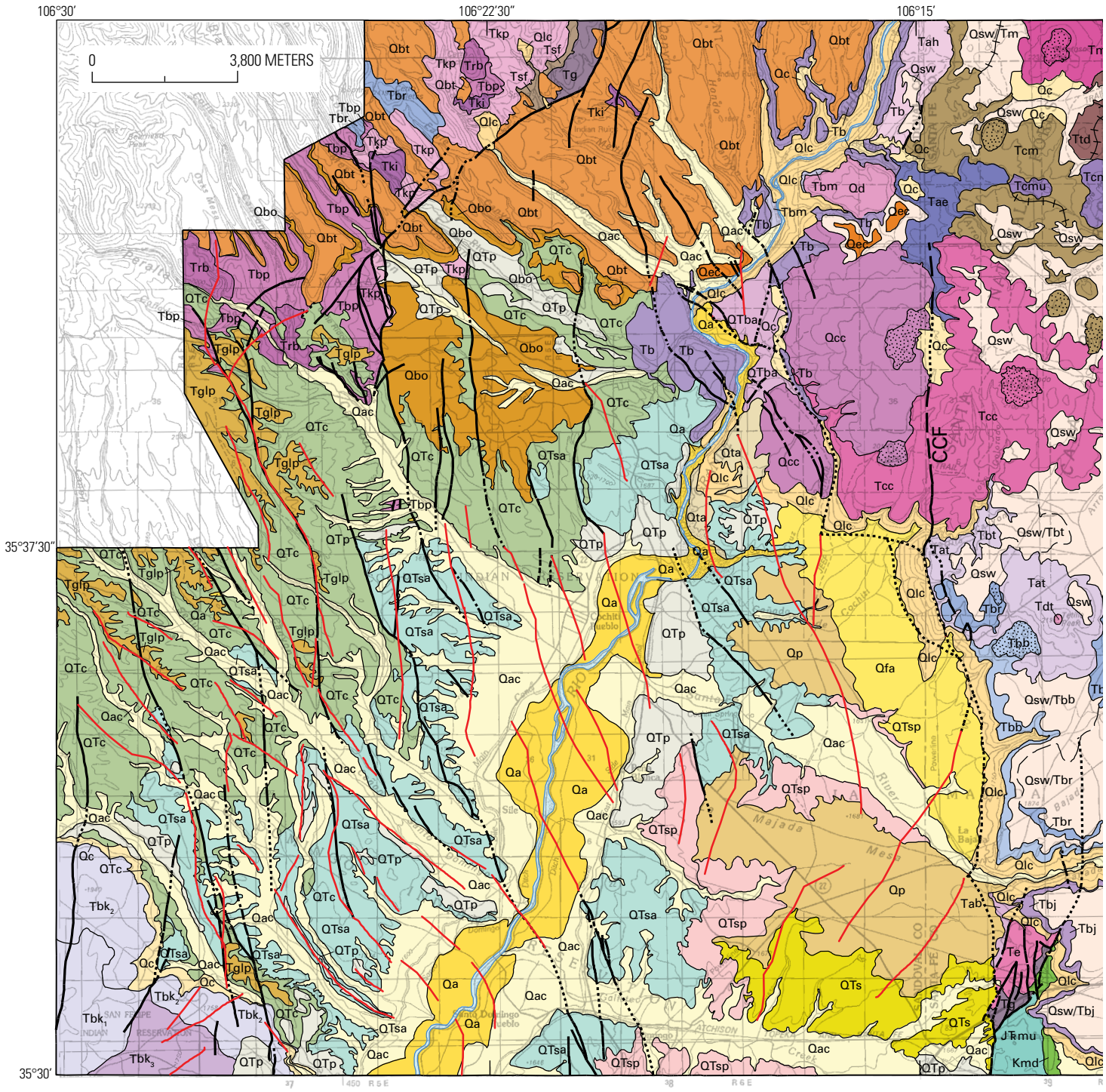

LIST OF MAP UNITS IN LA BAJADA CONSTRICTION REGION

[Units not listed in stratigraphic order within each geologic period]

QUATERNARY

Qc	Colluvium, undivided	Qp	Young pediment deposits	Qsw/Tbs	Sheetwash deposits over basalt of Tsinat Mesa
Qa	Flood-plain and stream-channel deposits	Qsw	Sheetwash deposits—Underlying Tertiary basalt unit indicated where mapped	Qsw/Tbt	Sheetwash deposits over basalt of Tetilla Hole
Qac	Alluvium and colluvium, undivided	Qsw/Tbb	Sheetwash deposits over basalt of La Bajada	Qsw/Tm	Sheetwash deposits over basaltic andesite of Cerro Montoso
Qfa	Fan alluvium	Qsw/Tbj	Sheetwash deposits over basalt of Mesita de Juana Lopez	Qta	Terrace and alluvial deposits
Qlc	Landslide and colluvial deposits, undivided	Qsw/Tbr	Sheetwash deposits over basalt of Caja del Rio	Qec	El Cajete tephra

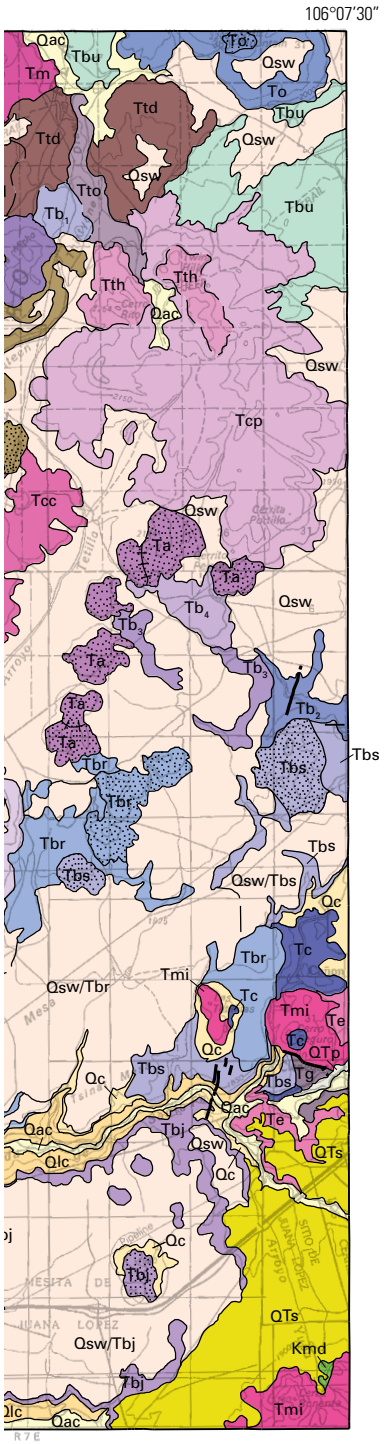

Bandelier Tuff
- Qbt — Tshirege Member
- Qbo — Otowi Member
- Qcc — Basaltic andesite of Cochiti Cone
- Qd — Dacite of White Rock Canyon
- QTba — Basalt of Cochiti
- QTp — Old pediment deposits
- QTs — Upper part of Santa Fe Group, undivided

Sierra Ladrones
- QTsa — Axial river facies
- QTsp — Eastern piedmont facies
- QTc — Cochiti Formation

TERTIARY
- Tglp — Gravel of Lookout Park
- To — Andesite of Ortiz Mountain
- Ttd — Basaltic andesite of Tank 31
- Tth — Andesite of Twin Hills
- Tto — Basalt of Thirty One Draw
- Tae — Andesite of Arroyo Eighteen
- Tah — Andesite of Hill 6385

Flows of Bajada Mesa
- Tb_4 — Upper basalt
- Tb_3 — Lower basalt
- Tb_2 — Basaltic andesite of Petroglyph Canyon
- Tb_1 — Basalt of Hill 7071

Basalt of Santa Ana Mesa
- Tbk_3 — Upper basalt
- Tbk_2 — Middle basalt
- Tbk_1 — Lower basalt
- Ta — Late andesite of Caja del Rio
- Tbr — Basalt of Caja del Rio
- Tbt — Basalt of Tetilla Hole
- Tbu — Basalt of Canada Ancha
- Tm — Basaltic andesite of Cerro Montoso
- Tcc — Andesite of Cerro Colorado
- Tcmu — Late andesite of Cerro Micho
- Tcm — Basaltic andesite of Cerro Micho
- Tcp — Andesite of Cerro Portrillo
- Tb — Basalt of White Rock Canyon
- Tat — Andesite of Tetilla Peak
- Tdt — Dacite of Tetilla Peak
- Tbj — Basalt of Mesita de Juana Lopez
- Tbb — Basalt of La Bajada
- Tbs — Basalt of Tsinat Mesa
- Tbm — Hydromagnetic deposits of White Rock Canyon
- Trb — Bearhead Rhyolite
- Tbp — Peralta Tuff Member of Bearhead Rhyolite
- Tki — Intrusive dacite of Paliza Canyon Formation
- Tkp — Paliza Canyon Formation, undivided
- Tsf — Middle part of Santa Fe Group, undivided
- Tab — Abiquiu(?) Formation
- Tc — Cieneguilla Basanite
- Te — Espinaso Formation
- Tmi — Monzonite and monzonite porphyry
- Tg — Galisteo Formation

CRETACEOUS
- Kmd — Mancos Shale and Dakota Sandstone, undivided

JURASSIC
- JTrmu — Morrison, Wanakah, Entrada, Todilto, and Chinle Formations, undivided

- **Cinder deposits**—Formed during same eruptive event as underlying flow
- **Contact**—Dashed where approximately located
- **Magnetic boundary**—Abrupt difference in rock-magnetic properties inferred from aeromagnetic data
- **Fault inferred from aeromagnetic data**
- **Fault**—Offset unknown. Dashed where approximately located; dotted where concealed. CCF, Cochiti Cone fault

Figure C2 (above and facing page). Geology of the La Bajada constriction area (scale 1:125,000) emphasizing volcanic deposits; modified from geologic map shown on plate 2. Geologic map data from Spiegel and Baldwin (1963); Smith, Bailey, and Ross (1970); Bachman (1975); Kelly and Kudo (1978); Goff, Gardner, and Valentine (1990); Dethier (1997); Smith and Kuhle (1998a,b); Sawyer and others (2002); and mapping by R.A. Thompson (unpub. data, 2005), R.R. Shroba (unpub. data, 2005), and D.P. Dethier (unpub. data, 2005).

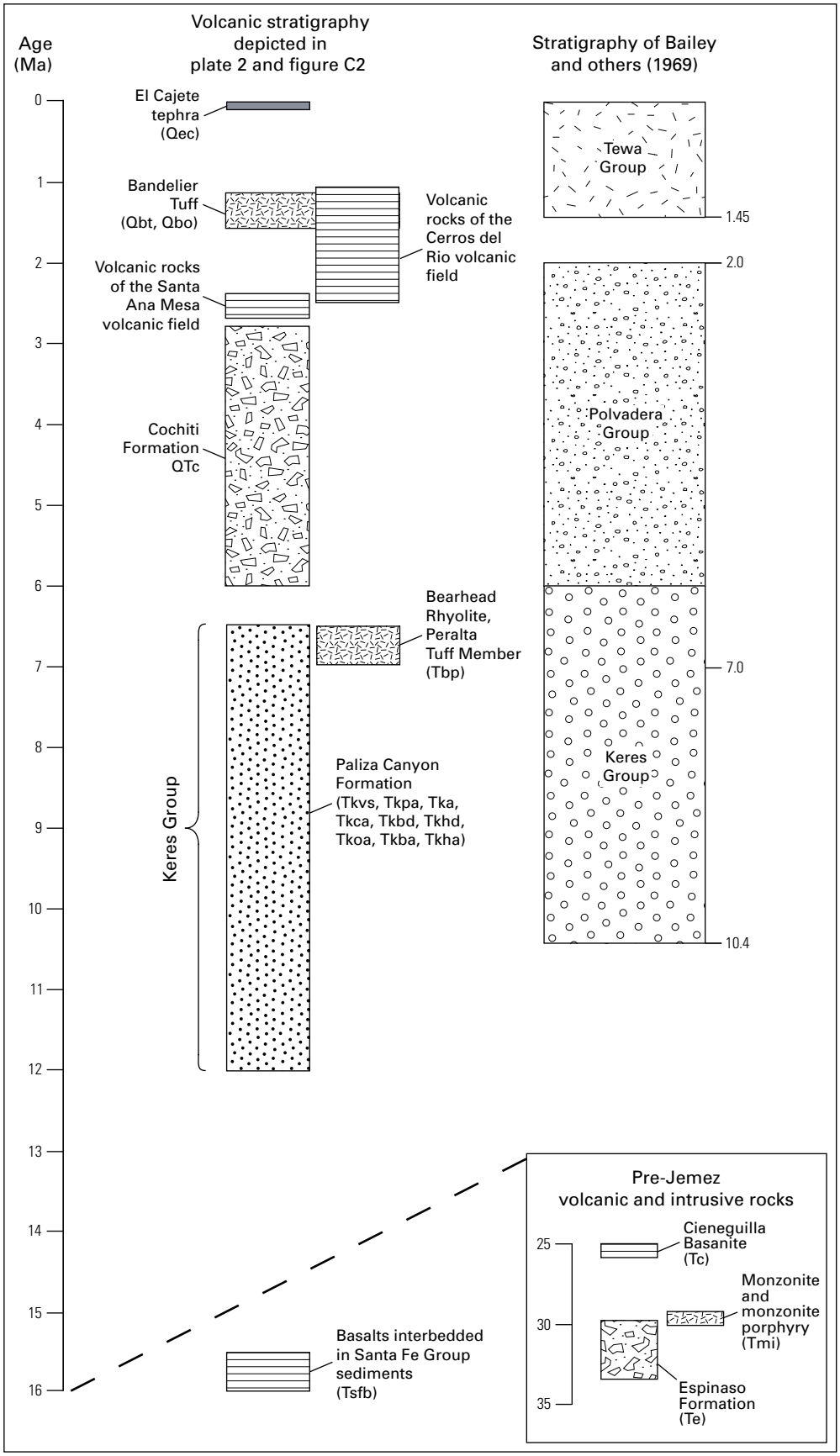

Figure C3. Generalized stratigraphic relations for the La Bajada constriction region. Published data sources include Bailey, Smith, and Ross (1969); Gardner and others (1986); Lavine, Smith, and Goff (1996); WoldeGabriel and others (1996); G.A. Smith (personal commun., 2002); and mapping by R.A. Thompson (unpub. data, 2005), R.R. Shroba (unpub. data, 2005), and D.P. Dethier (unpub. data, 2005).

Pre-Rift Tertiary Volcanism

Exposures of pre-rift middle Tertiary intrusions, volcanic rocks, and volcaniclastic sedimentary deposits are confined to the southeastern part of the map area (pl. 2, fig. C2). They form the bedrock under a broad, irregular paleoerosion surface upon which Pliocene rocks of the Cerros del Rio volcanic field and basin-fill sediments of the Santa Fe Group were deposited. The Espinaso Formation (unit Te, pl. 2, fig. C2), northern Cerrillos Hills intrusions (unit Tmi), and Cieneguilla volcanic complex (unit Tc, Cieneguilla Basanite) are confined to the footwall block of the La Bajada fault zone. Existing radiometric ages for these rocks are poorly constrained and range from late Eocere to early Miocene. These ages suggest that the volcanism likely was associated with the transition from post-Laramide arc volcanism (related to subduction) to early extensional volcanism (related to rifting) as recognized elsewhere in uplifted rift margins in northern New Mexico and southern Colorado (Thompson, Dungan, and Lipman, 1986; Lipman, 1988; Thompson, Johnson, and Mehnert, 1991, Miggins and others, 2002)

The Espinaso Formation is composed of andesite lava flows and volcaniclastic breccias that are unconformably overlain by two separate dacite flow sequences with interbedded volcaniclastic sedimentary rocks. Sun and Baldwin (1958) reported K-Ar age determinations of 19.5±0.5 and 19.6±0.6 Ma on biotite and feldspar, respectively, collected from the upper dacite lava flow. These ages might not be primary because they are younger than ages reported for the overlying Cieneguilla lava flows and because the upper dacite is similar in composition and mineralogy to the youngest of the Cerrillos Hills intrusions (36–31 Ma) to the southeast (Sawyer and others, 2002).

Eocene and Oligocene intrusive rocks of the Cerrillos Hills in the Cochiti Pueblo map area (unit Tmi, pl. 2, fig. C2) consist of fine-grained, subvolcanic stocks and dikes of monzonite and monzonite porphyry. These rocks are exposed at Cerro Bonanza, Cerro Seguro, Las Tetillitas, and within Cañada de Santa Fe (pls. 1, 2). The augite monzonite porphyry of Cerro Seguro is compositionally similar to the stratigraphically highest dacites of the Espinaso Formation. Baldridge and others (1980) reported a K-Ar biotite age of 30.2±0.7 Ma and, more recently, Sauer (1999) obtained a 29.40±0.05-Ma $^{40}Ar/^{39}Ar$ plateau age on biotite for the monzonite of Cerro Seguro. This intrusion domed flanking deposits of the Galisteo Formation (unit Tg) and the lower part of the Espinaso Formation (unit Te) near Cañada de Santa Fe; thus, these deformed deposits must be considerably older than previously reported by Sun and Baldwin (1958). Disbrow and Stoll (1957) tentatively correlated the Cerro Seguro intrusions with late stage Cerrillos Hills intrusive activity.

Rocks of the Cieneguilla volcanic complex (Cieneguila Basanite), which conformably overlie the Espinaso Formation, consist of basanite and nephelenite lava flows and interbedded volcaniclastic and epiclastic sediments (Sterns, 1953; Sun and Baldwin, 1958; Baldridge, 1979b; Baldridge and others, 1980). These deposits overlie the Espinaso Formation in Cañada de Santa Fe and south of the Mesita de Juana Lopez vent (fig. C2). The sequence is as thick as 200 m and contains four discrete packages of lava flows, each containing as many as five discontinuous lava flows, basaltic tephra, and interbedded volcaniclastic sediments. Baldridge and others (1980) reported a whole-rock K-Ar age of 25.1±0.7 Ma on a lava-flow sequence that assumes the same regional northeasterly dip as the underlying Espinaso Formation. North- to northeast-trending dikes of similar composition cut older rocks in the footwall of the La Bajada fault south of Cañada de Santa Fe (Sawyer and others, 2002).

Jemez Volcanic Field

The Jemez Mountains host a spectacular example of a long-lived, large-volume, compositionally varied volcanic field that culminated in caldera-forming eruptions of silicic ignimbrites; this field has been the subject of studies on the nature of caldera-forming process and the emplacement mechanisms of rhyolite ash-flow tuffs (Smith and Bailey, 1966, 1968). Geologic and hydrologic framework investigations also established a regional stratigraphic nomenclature (Griggs, 1964; Bailey, Smith, and Ross, 1969; Smith, Bailey, and Ross, 1970). Subsequent investigations, supported by large-scale mapping and additional radiometric age determinations, have led to revisions of the original nomenclature, particularly as applied to precaldera and postcaldera eruptive units (Gardner and others, 1986; Lavine, Smith, and Goff, 1996; Reneau, Gardner, and Forman, 1996).

In the La Bajada constriction area, within the highlands of the Pajarito Plateau, precaldera deposits are largely concealed beneath the Otowi and Tshirege Members of the Pleistocene Bandelier Tuff, erupted during collapse of the Jemez caldera (pl. 2, fig. C2). Consequently, exposures of precursory basaltic to rhyolitic volcanic rocks are limited to the dissected footwall block of the Pajarito fault zone (that is, the Saint Peters Dome block, fig. A2) and southeastern slopes of the precaldera eruptive surface. With the exception of deposits associated with basaltic volcanism of the Cerros del Rio volcanic field, postcaldera volcanic deposits in the La Bajada constriction area are limited to reworked pumice and ash deposits of the approximately 50-ka El Cajete tephra (unit Qec, pl. 2, figs. C2, C3) (Reneau, Gardner, and Forman, 1996; Reneau, McDonald, and others, 1996; Wolf, Gardner, and Reneau, 1996). This pumice and ash blanket the northeastern slopes of eroded volcanic highlands east of the Rio Grande.

All precaldera volcanic and volcaniclasitic deposits of the Pajarito Plateau (pl. 1) belong to the Keres Group as defined by Bailey, Smith, and Ross (1969) and modified by Gardner and others (1986). The Keres Group rests unconformably on Santa Fe Group sediments (unit Tsf, pl.2) and locally on 16-Ma basaltic lava flows (unit Tsfb) related to rifting (Goff, Gardner, and Valentine, 1990). The Keres Group consists predominantly of andesite to dacite lavas, pyroclastic deposits,

volcanic breccias, and sedimentary deposits (Gardner and others, 1986; Lavine, Smith, and Goff, 1996). Age of the volcanic rocks ranges from approximately 12 Ma near the base of the Paliza Canyon Formation to approximately 6.5 Ma, the youngest age reported for the Bearhead Rhyolite; most volcanism occurred between 10 and 8 Ma (Gardner and others, 1986; McIntosh and Quade, 1995; Lavine, Smith, and Goff, 1996; Justet, 1999).

In the La Bajada constriction area near Saint Peters Dome (pl. 2, fig. A2), Keres Group rocks are dominated by andesite and dacite lava flows, domes, and minor intrusives (units Tkha, Tkba, Tkoa, Tkhd, Tkbd, Tkca, Tka, Tkpa; pl. 2); they extend westward underneath the Pajarito Plateau and crop out in the highlands of the San Miguel Mountains. Local olivine basalt lava flows and cinder deposits are found near the base and top of the section (Goff, Gardner, and Valentine, 1990). Collectively, these deposits compose the Paliza Canyon Formation.

The youngest eruptive products included in the Keres Group are the isolated high-level intrusions of Bearhead Rhyolite (unit Trb, pl. 2) (Smith, Bailey, and Ross, 1970; Goff, Gardner, and Valentine, 1990) and associated Peralta Tuff Member of the Bearhead Rhyolite (unit Tbp) (figs. C2, C3). The sparsely phyric Bearhead Rhyolite occurs as localized lava domes and as flows and their pyroclastic aprons, emplaced during two discrete, short-lived intervals between 7 Ma and 6.5 Ma (G. Smith, personal commun., 2002). The Peralta Tuff Member of the Bearhead Rhyolite comprises pyroclastic flow, fall, and surge deposits related to localized emplacement of lava domes. In the footwall block of the Pajarito fault zone (pl. 2), the Paliza Canyon Formation is locally intercalated with compositionally similar deposits of the Canovas Canyon Formation (units Tkct, Tkrc).

The Cochiti Formation (unit QTc, pl. 2) contains volcaniclastic detritus shed from the volcanic highlands of Keres Group volcanic centers (Smith, Bailey, and Ross, 1970; Goff, Gardner, and Valentine, 1990). Locally, it may instead contain temporally and spatially equivalent primary volcanic deposits. Lavine, Smith, and Goff (1996) proposed a more restrictive use of the term "Cochiti Formation" to include only those sedimentary deposits that postdate emplacement of the Bearhead Rhyolite lavas and pyroclastic deposits of the Peralta Tuff Member. As such, the Cochiti Formation as depicted in plate 2 and figure C2 represents a temporal equivalent to other upper Santa Fe deposits of the Santo Domingo and Española Basins. The Cochiti Formation is discussed in more detail in the context of basin-fill sedimentary deposits in chapter B (this volume).

Santa Ana Mesa Volcanic Field

Bryan (1938) and Kelly and Kudo (1978) used the term "San Felipe volcanic field" to refer to the basaltic lavas that capped Santa Ana Mesa north of the confluence of the Jemez River and the Rio Grande (pl. 1). Subsequently, Baldridge (1979a) and Personius (2002) referred to the same lavas as the Santa Ana Mesa volcanic field (SAMVF, figs. C1, A2). In the northeastern portion of this volcanic field lava flows and associated pyroclastic deposits form a succession of chemically and mineralogically similar olivine tholeiites (Baldridge, 1979a) erupted from low-relief shield volcanoes and small, late-stage cinder cones (units Tbk_1, Tbk_2, Tbk_3; pl. 2, fig. C2). Basal lava flows form a broad plateau erupted onto a low-relief erosional surface cut into sediments of the Santa Fe Group (unit QTsa) and Cochiti Formation (unit QTc). Hydromagmatic deposits and basaltic tuffs lie at the base of the volcanic succession and are similar in character to those observed in the Cerros del Rio volcanic field. K-Ar ages (Kelly and Kudo, 1978; Bachman and Mehnert, 1978) and $^{40}Ar/^{39}Ar$ ages (Smith and Kuhle, 1998a,b) on the lava flows range from 2.6 to 2.4 Ma. North-striking normal faults displace the Santa Ana Mesa flows (fig. E1) by as much as 100 m, and similar faults may have exerted synvolcanic structural control on magma conduits as evidenced by the predominant north-trending alignment of cinder cones delineating late-stage vent areas.

Cerros Del Rio Volcanic Field

The Cerros del Rio volcanic field (CDRVF; pl. 1, figs. C1, A2) is a predominantly basaltic to andesitic volcanic plateau in the La Bajada constriction area. This field is bounded on the southwest by the La Bajada fault zone (pl. 1, fig. A4), forms a topographic high, and is overlain by Española Basin fill deposits to the north and east; Pleistocene ash-flow tuffs of the Jemez volcanic field abut the northwest margin of this high (fig. C2). Pliocene to Quaternary volcanic rocks of the Cerros del Rio field overlie much of the La Bajada constriction, obscuring the stratigraphic and structural link between the Española and Santo Domingo Basins (fig. A2; chapter G, this volume). Lavas and related pyroclastic deposits of this field have a surface expression of 700 km^2 and reflect eruption of at least 120 km^3 of rift-related mafic magma. Most of the lava flows predate large-volume silicic eruptions of the Jemez volcanic field; however, late stage eruptions from the field postdate eruption of the Bandelier Tuff. Eruptive centers in this field are typically central-vent volcanoes ranging from low-relief shields to steep-sided, breached cinder cone remnants. Lavas range from 48 to 65 wt percent SiO_2 (fig. C4); their geomorphic expression strongly correlates with their whole-rock chemistry. Low-silica, subalkaline basaltic lavas are thin (<3–4 m), were erupted from broad shield volcanoes, and traveled long distances, whereas transitional to mildly alkaline basalts and basaltic andesites form thick (as much as 30 m thick), discontinuous lava flows and were erupted from high-relief, steep-sided, dissected vents. Dacitic lavas are related to late-stage dome growth and eruption of thick (as much as 50 m thick) blocky lava flows from one well-defined vent area at Tetilla Peak (TP, pl. 1) and also form lava flows exposed in tributary canyons of White Rock Canyon (pl. 1).

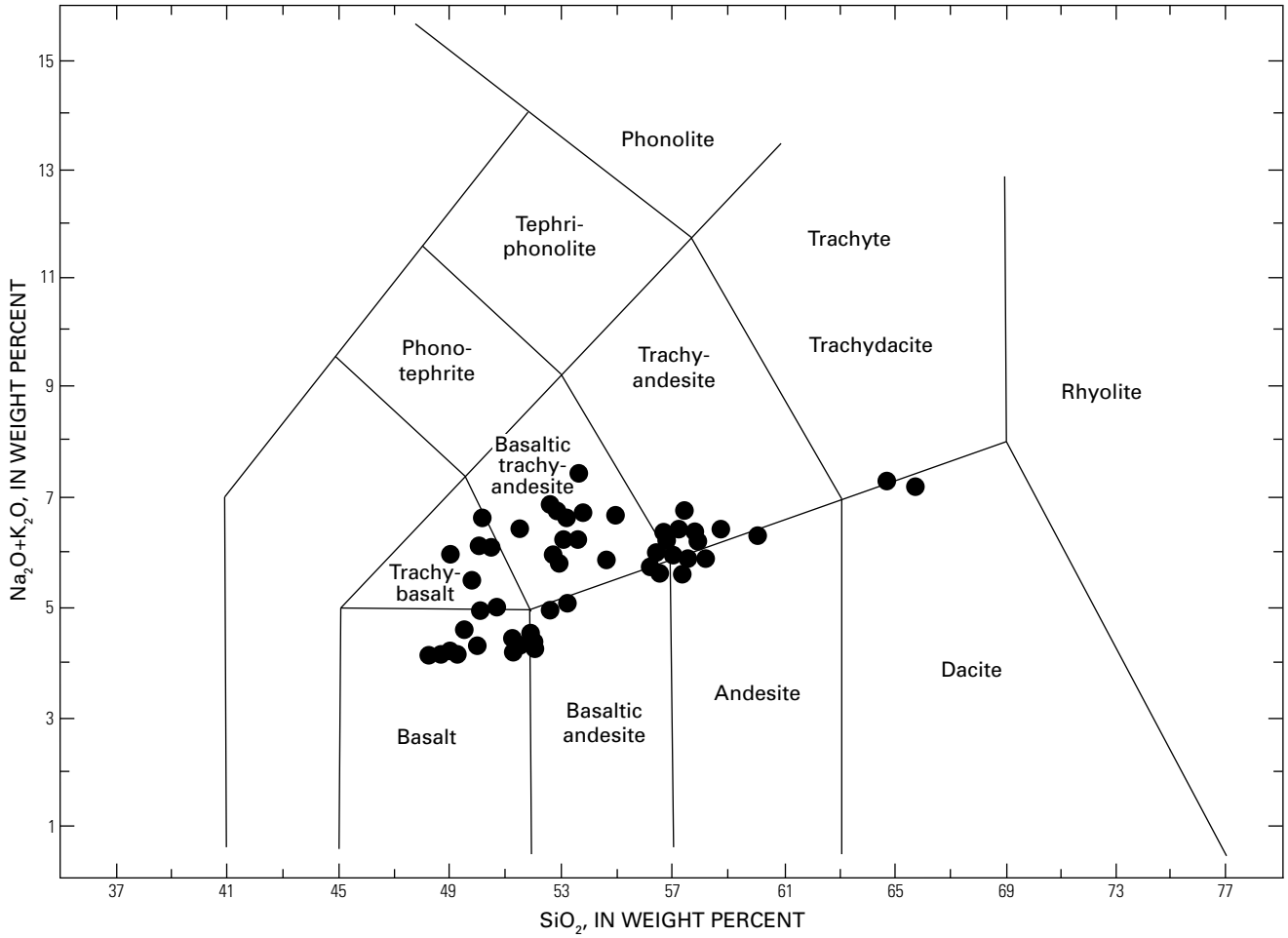

Figure C4. Total alkali versus silica for select Cerros del Rio volcanic rock samples. Diagram illustrates the range of chemical compositions represented by early-, middle-, and late-phase eruptions. Classification and fields based on Le Bas and others (1986).

Previous regional investigations identified the areal extent, stratigraphic position, broad compositional spectrum, and geochronologic constraints of the Cerros del Rio lavas (Spiegel and Baldwin, 1963; Smith and others, 1970; Aubele, 1978; Bachman and Mehnert, 1978; Aubele, 1979; Baldridge, 1979a). More recent stratigraphic and geochronologic control from Cerros del Rio volcanic field lavas exposed on the Pajarito Plateau (pl. 1) and in western White Rock Canyon are summarized in WoldeGabriel and others (1996, 2001), and petrologic constraints on the evolution of limited suites of Cerros del Rio lavas were presented in Zimmerman and Kudo (1979), Dunker and others (1991), and Wolfe, Heikoop, and Ellisor (2000).

The geologic map relations for the Cerros del Rio volcanic field presented in figure C2 and plate 2 are based on mapping investigations by Aubele (1978), Dethier (1997), and Sawyer and others (2002) and on maps by R.A. Thompson and D.P. Dethier (unpub. data, 2005). Volcanic deposits of the central, southern, and western Cerros del Rio were mapped at 1:24,000 scale and simplified for presentation at 1:125,000 scale (fig. C2). All of the volcanic unit names are informal, with the exception of the Otowi and Tshirege Members of the Bandelier Tuff. Volcanic units delineate monogenetic eruptive centers where possible; however, simplification from the original mapping dictates consolidation of map units on the basis of lithologic character, stratigraphic position, age, aeromagnetic and paleomagnetic signature, and aerial extent of similar or related deposits.

Thickness of the volcanic pile ranges considerably from a maximum exposed thickness of approximately 100 m in White Rock Canyon to a few meters along the eastern margin of the field. Along the eastern margin, lava flows and basaltic hydromagmatic deposits dip gently beneath basin-fill deposits of the Ancha Formation (Grauch and Bankey, 2003). Driller's records from the 1200-Foot well in the south central part of the Cerros del Rio volcanic field (pl. 2) indicate approximately 240 m of basaltic lava flows, pyroclastic deposits, and interbedded alluvium (fig. G2). Projected thicknesses for the entire volcanic field are represented in a set of serial cross sections on plate 6.

Aerial Distribution, Geochronology, and Geochemistry

Volcanic deposits of the Cerros del Rio volcanic field are divided into a threefold classification representing early, middle, and late phases of eruption spanning approximately 2.7–1.1 Ma (fig. C5, table C1). These subdivisions are based on 1:24,000-scale geologic mapping, stratigraphic studies, $^{40}Ar/^{39}Ar$ geochronology, and paleomagnetic and aeromagnetic data. Limited geochemical data were used to classify lithologic types within the stratigraphic subdivisions but were not used to infer stratigraphic position. Results of new $^{40}Ar/^{39}Ar$ age determinations are presented in figure C5 and table C1, and a total alkali versus silica geochemical classification diagram using the scheme of Le Bas and others (1986) is presented in figure C4.

Early-phase eruptions produced areally extensive, large-volume, plateau-forming lava flows ranging in age from 2.7 to 2.6 Ma (fig. C5). They form much of the La Bajada escarpment, prominent cliffs of northern White Rock Canyon, and the southeastern margin of the volcanic field (fig. C2). Vents associated with these lava flows characteristically are large composite cinder cones, such as the topographically prominent peaks at Mesita de Juana (unit Tbj), Cerro Montoso (unit Tm), Cerro Colorado (unit Tcc), and unnamed source areas for the basalt of La Bajada (unit Tbb) and basalt of Tsinat Mesa (unit Tbs) (pl. 2, fig. C2). These centers and their associated lava flows are predominantly basalt to basaltic andesite (fig. C4). Evolved dacite compositions for early-phase eruptions were limited to late emplacement of a small lava dome at Tetilla Peak (unit Tdt). This lava dome was emplaced after eruption of pyroxene-plagioclase-hornblende andesites from the same Tetilla Peak vent area (unit Tat).

Middle-phase volcanism was less extensive and was typified by smaller eruptive volumes than early-phase eruptions. However, the eruptive interval for middle-phase activity was at least twice as long as that observed for the early phase as implied by $^{40}Ar/^{39}Ar$ age determinations ranging from 2.5 to 2.2 Ma (fig. C5). Map units depicted in figure C2 illustrate complex stratigraphic relations resulting from three primary factors. First, individual eruptive centers yielded highly variable eruption volumes and not all map units have known vent areas. Second, fluvial erosional topography developed on the surface of early-phase flows before resulting canyons were filled by middle-phase lava flows, and inverted stratigraphy resulted. Third, the morphology of vents and flows is variable and reflects the compositional variation (from basaltic to andesitic) of lava erupted from middle-phase volcanoes. Andesite volcanoes form discrete, high-relief centers (units To, Tcp; fig. C2), whereas smaller volume basalt and basaltic-andesite centers are typified by smaller eruptive volumes, widespread distribution of basaltic to basaltic andesite lava flows, and multiple vent areas likely associated with fissure eruption (units Tcm, Tcmu, Ta, Tb_1, Tb_2, Tb_3, Tb_4, Ttd, Tto). In all cases, flow morphology of individual centers reflects the relative silica content and consequently the viscosity of eruptive products.

Figure C5 (facing page). $^{40}Ar/^{39}Ar$ ages and associated ±2σ analytical errors (vertical bars) of volcanic rocks of the Cerros del Rio volcanic field plotted relative to the magnetic geochron for the time period 2.96–1.00 Ma; inset shows age control and magnetic geochron for late-phase Quaternary volcanic rocks of the time period 1.48–1.00 Ma. Map unit symbols in parentheses defined in Explanation on figure C2. Polarity of unit interpreted from aeromagnetic data listed to right of unit symbol. Sample locations shown on plate 2 and listed in table C1. Map unit symbols: Qcc, basaltic andesite of Cochiti Cone; Qd, dacite of White Rock Canyon; QTba, basalt of Cochiti; Tb, basalt of White Rock Canyon; Tb_2, basaltic andesite of Petroglyph Canyon; Tb_3, lower flow unit of Bajada Mesa; Tbb, basalt of La Bajada; Tbj, basalt of Mesita de Juana Lopez; Tbs, basalt of Tsinat Mesa; Tbt, basalt of Tetilla Hole; Tcc, andesite of Cerro Colorado; Tm, basaltic andesite of Cerro Montoso; To, andesite of Ortiz Mountain.

Eruptive products from late-phase volcanoes are restricted to a narrow corridor west of the Cochiti Cone fault (CCF, fig. C2) and east of the Rio Grande in lower White Rock Canyon (pl. 1). Three primary eruptive centers (units Qcc, Qd, QTba; fig. C2) have been identified and range in age from approximately 1.5 to 1.1 Ma (fig. C5). In White Rock Canyon, all three volcanoes locally overlie erosional remnants of the Tshirege Member of the Bandelier Tuff, and the youngest eruptions from Cochiti Cone (unit Qcc) locally overlie the Otowi Member of the Bandelier Tuff. Lavas from the two oldest of these volcanoes (units QTba, Qd) overlie middle-phase basaltic andesites (unit Tb) in White Rock Canyon, and deposits from multiple vents of the Cochiti Cone volcano overlie both early-phase (unit Tcc) and middle-phase (unit Tb) lava flows in White Rock Canyon and along the La Bajada escarpment (fig. C2). Compositions of late-phase lavas are predominantly basaltic andesite, but evolved dacite compositions were erupted from the northernmost (unit Qd) of the three centers in White Rock Canyon.

Table C1. New $^{40}Ar/^{39}Ar$ age determinations from Cerros del Rio volcanic field.

[Map unit symbols as depicted in fig. C2]

Sample number	Map unit symbol	Latitude (°N)	Longitude (°W)	Age (Ma)	±2σ analytical error (Ma)
96DTP05	Tbr	35.56211	106.21927	2.35	0.06
96DTP12	Tbr	35.61245	106.17496	2.42	0.03
96DTP13	Tbj	35.52126	106.20072	2.66	0.08
96DTP19	Tbb	35.60031	106.23528	2.61	0.14
96DTP24	Tbr	35.60642	106.23145	2.44	0.06
96TCD01	Tbb	35.63425	106.25990	2.67	0.05
DN85113	Qd	35.71800	106.27100	1.31	0.08
DN9628b	QTba	35.63224	106.29850	1.46	0.06
96TCD08	Qcc	35.64658	106.27849	1.14	0.13
96TMP08	Tm	35.73605	106.21491	2.59	0.05
96TMP09	Tb_3	35.64588	106.16958	2.19	0.13
96TMP14	To	35.73797	106.14033	2.32	0.06
96TMP22	Tbt	35.63330	106.22938	2.49	0.05
96TMP38	Tcc	35.66350	106.21941	2.60	0.10
96TMP43	Tb_2	35.62990	106.13520	2.50	0.06

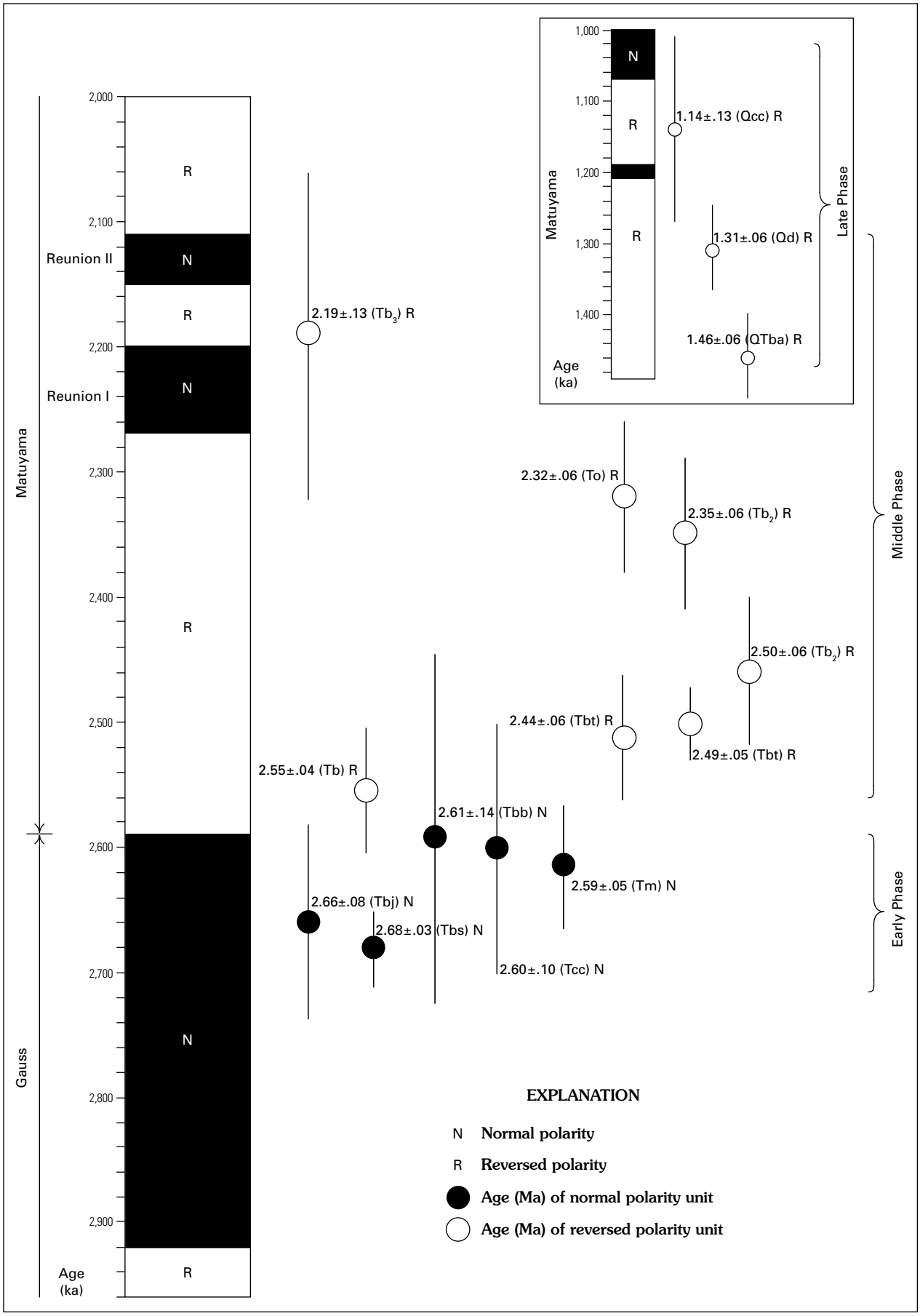
Matuyama
Gauss
Reunion II
Reunion I
Age (ka)
2,000
2,100
2,200
2,300
2,400
2,500
2,600
2,700
2,800
2,900
R
N
R
N
R
N
R
Matuyama
Age (ka)
1,000
1,100
1,200
1,300
1,400
N
R
R
1.14±.13 (Qcc) R
1.31±.06 (Qd) R
1.46±.06 (QTba) R
Late Phase
2.19±.13 (Tb3) R
2.32±.06 (To) R
2.35±.06 (Tb2) R
2.50±.06 (Tb2) R
2.44±.06 (Tbt) R
2.49±.05 (Tbt) R
2.55±.04 (Tb) R
2.61±.14 (Tbb) N
2.59±.05 (Tm) N
2.66±.08 (Tbj) N
2.68±.03 (Tbs) N
2.60±.10 (Tcc) N
Middle Phase
Early Phase
EXPLANATION
N Normal polarity
R Reversed polarity
Age (Ma) of normal polarity unit
Age (Ma) of reversed polarity unit

Magnetic Polarities

The aeromagnetic expression of volcanic rocks is commonly dominated by remnant magnetization. Volcanic rocks with strong, reverse-polarity, remnant magnetization produce distinctive, high-amplitude negative anomalies, whereas normal-polarity remnant magnetization produces high-amplitude positive anomalies (chapter D, this volume). Recognition of these distinctive anomalies in relation to mapped volcanic rock units, combined with paleomagnetic measurements, can be used to locate flow contacts, determine areal flow extent, and assign ages to undated rock units.

Aeromagnetic data for the Cerros del Rio volcanic field were compiled from two surveys flown with 400-m and 150-m line spacings and observation heights of 73 m and 150 m above ground, respectively. The data were analytically continued to a common observation surface 100 m above ground, merged, and reduced to pole (chapter D, this volume). Aeromagnetic signatures of the Cerros del Rio volcanic field express many small, mostly negative, magnetic anomalies of large amplitude, relating to magnetizations inherited during cooling of individual lava flows and associated pyroclastic deposits. Magnetic anomalies correlate well with preliminary paleomagnetic site means for the volcanic field showing both reversed and normal magnetic polarities corresponding with signatures of both Gauss and Matuyama magnetic chrons. On plate 5, geologic map data derived from figure C2 are overlaid on a shaded-relief version of the reduced-to-pole aeromagnetic data, and paleomagnetic sample sites and polarities are shown. A summary of paleomagnetic site means for selected samples of the Cerros del Rio volcanic field is illustrated in figure C6, and paleomagnetic data for selected samples are presented in table C2. The errors associated with $^{40}Ar/^{39}Ar$ age determinations (fig. C5) preclude assignment of mapped lithologic units to magnetic chrons or subchrons solely on the basis of geochronology. However, magnetic properties in conjunction with age distributions and observed stratigraphic relations have proven useful in delineating map units and assigning them to major eruptive phases.

Early-phase eruptions were confined to the latest Gauss magnetic chron (figs. C5, C7) and are characterized by moderate to strong normal polarity signatures (plate 5) supported by normal paleomagnetic site means for units Tat, Tbs, Tbj, Tm, and Tbb (fig. C6). It is likely that much of the plateau is underlain by younger phases of Cerros del Rio volcanic rocks that produce strong negative magnetic polarities, and it is unclear what effect this polarity signature may have on thinly veneered overlying units of variable age and polarity.

Most middle-phase eruptions occurred during the early Matuyama magnetic chron but appear, on the basis of geochronology and magnetic properties, to extend into the Reunion subchrons (fig. C5). Early eruptive units within this phase, for example Tbt, Tb_2, and To, have $^{40}Ar/^{39}Ar$ ages ranging from 2.49 to 2.32 Ma, and their strong reversed aeromagnetic polarities are corroborated by reversed paleomagnetic site means for units Tbt and To. Units Tto, Tbb, Tb, and Tbr occur

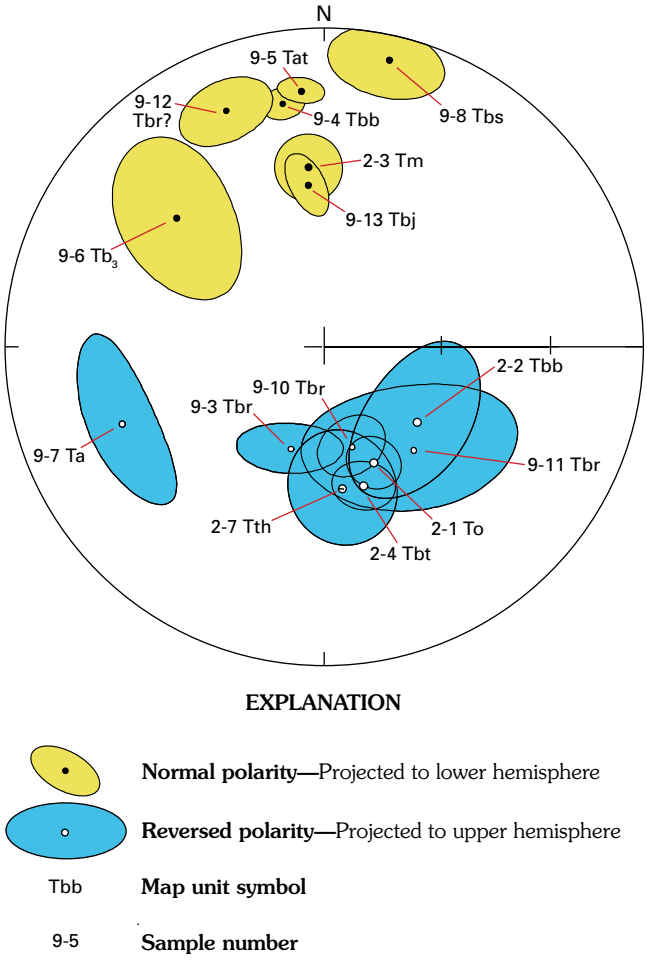

Figure C6. Paleomagnetic site mean directions for selected samples from the Cerros del Rio volcanic field (sample locations shown on pl. 5). Dots are projections onto an equal-area stereo diagram. Colored ovals about site mean directions are cones of 95 percent statistical confidence. Samples for paleomagnetic analysis collected by use of a portable rock drill and oriented by use of magnetic and solar compasses and a clinometer. In the laboratory, natural remanent magnetization of samples was measured using a spinner magnetometer. All samples were subjected to progressive alternating-field demagnetization, typically with nine or more steps, to peak fields of 100–200 nT. Most samples affected to some degree by secondary magnetizations imparted by lightning, and thus data from remagnetization circles (Halls, 1976) commonly were combined with best-fit linear directions (Kirschvink, 1980) to define site mean directions. Site means and dispersion parameters (table C2) calculated using Bingham statistics (Onstott, 1980) or Fisher statistics (Fisher, 1953). Map unit symbols: Ta, late andesite of Caja del Rio; Tat, andesite of Tetilla Peak; Tb_3, lower flow unit of Bajada Mesa; Tbb, basalt of La Bajada; Tbj, basalt of Mesita de Juana Lopez; Tbr, basalt of Caja del Rio; Tbs, basalt of Tsinat Mesa; Tbt, basalt of Tetilla Hole; Tm, basaltic andesite of Cerro Montoso; To, andesite of Ortiz Mountain; Tth, andesite of Twin Hills.

Table C2. Paleomagnetic data from Cerros del Rio volcanic field.

[Latitude and Longitude referenced to 1927 North American datum; Xo, site average magnetic susceptibility (SI volume unit of measure); N/No., ratio of number of samples accepted to number of samples demagnetized; Decl., Incl., declination and inclination of site-mean directions; α95–1, α95–2, minimum and maximum axes of ellipse of 95 percent confidence cone about mean direction (Onstott, 1980); K1, K2, concentration parameters; Oval az., oval azimuth for confidence ellipse. Site means for 9MRG–4, 2MRG–5, and 2MRG–15 calculated using statistics of Fisher (1953) and have single values for confidence cone oval and concentration parameter and no oval azimuth value]

Site	Latitude (°N)	Longitude (°W)	Xo	N/No.	Decl. (°)	Incl. (°)	α_{95-1}	α_{95-2}	K1	K2	Oval az.
9MRG–3	35.5624	106.2193	2.28E–2	8/8	198	–62.3	6.77	13.59	–35.6	–2.8	72.8
9MRG–4	35.5516	106.2220	2.09E–2	6/8	350.5	24.4	5.01		179.8		
9MRG–5	35.6005	106.2028	2.98E–3	8/8	355.1	21.1	4.04	5.53	–117.6	–1.2	58.1
9MRG–6	35.6452	106.1707	3.31E–2	4/8	310.9	39	13.5	24.47	–19.7	–2.2	165.9
9MRG–7	35.6223	106.1818	3.48E–2	6/8	248.8	–32.8	10.01	21.09	–22.1	–2.8	85
9MRG–10	35.6081	106.1965	2.92E–2	8/10	164.3	–63.2	7.51	9.41	–30.4	–0.8	66.1
9MRG–11	35.5682	106.1635	3.22E–2	4/8	139.4	–54.8	16.37	27.75	–14.4	–1.8	129
9MRG–12	35.5661	106.1610	2.13E–2	8/8	337.4	21.6	9.55	10.66	–26	–0.4	103.4
9MRG–13	35.5213	106.2008	2.60E–2	6/8	354.3	48.2	4.37	9.45	–106.2	–3.3	18.1
2MRG–1	35.7392	106.1394	2.34E–2	8/8	156.7	–57.5	6.2	7.5	–37.5	–0.7	159.9
2MRG–2	35.7366	106.1393	3.27E–2	7/8	129.1	–59.2	13.8	21.7	–12.4	–1.5	84.1
2MRG–3	35.7369	106.2045	2.58E–2	9/9	355.0	42.9	7.9	9.4	–22.4	–0.6	2.5
2MRG–4	35.6328	106.2287	3.68E–2	8/8	164.2	–52.6	6.3	7.9	–47.2	–0.9	125.8
2MRG–5	35.6428	106.2267	3.59E–2	8/8	168.1	–59.6	3.9		198.8		
2MRG–6	35.7055	106.1700	1.20E–2	7/8	138.4	–68.6	5.1	6.1	–92.3	–0.7	34.2
2MRG–7	35.7065	106.1660	7.67E–3	8/8	172.7	–53.0	13.0	15.7	–10.7	–0.6	9.5
2MRG–8	35.6926	106.1637	7.02E–3	8/8	352.5	57.9	11.9	16.6	–15.1	–1.1	18.0
2MRG–11	35.6506	106.1732	2.87E–2	8/8	343.5	47.8	9.9	31.2	–15.9	–4.2	91.5
2MRG–12	35.6467	106.1761	1.20E–2	8/8	154.8	–63.2	6.2	11.6	–34.6	–2.4	37.9
2MRG–13	35.6565	106.1715	4.70E–3	8/8	348.6	47.7	4.2	4.9	–108.3	–0.6	8.1
2MRG–14	35.6562	106.1707	3.26E–2	7/8	332.8	57.1	8.7	15.4	–26.4	–2.1	47.2
2MRG–15	35.6397	106.1452	3.22E–2	7/8	160.5	–68.2	9.7		40.0		

in similar stratigraphic position and also possess negative aeromagnetic signatures, but they are undated. Units Tbr and Tbb have reversed paleomagnetic site means. Stratigraphically younger, undated units that possess normal aeromagnetic polarities include units Tcp, Tb_1, and Tcmu (fig. C7). It is stratigraphically permissible that these units were erupted during either the Reunion I or Reunion II normal excursions. This interpretation is supported by the observation that morphologically younger cinder cones (unit Tth, fig. C2) lying stratigraphically above unit Tcp possess strong reversed aeromagnetic signatures. A particularly problematic series of middle-phase deposits are represented by unit Ta. A series of morphologically similar, small, cinder cones belonging to this unit overlie a related lava flow dated by $^{40}Ar/^{39}Ar$ methods at 2.19±13 Ma. The overlying cinder cones have both negative and positive aeromagnetic signatures for short lateral distances unaccompanied by discernable lithologic or temporal variation in the deposits. It is permissible within the errors of existing age determinations that eruption intervals spanned magnetic reversals, perhaps many times, within the Reunion subchrons of the Matuyama and resulted in lithologically similar deposits with both positive and negative aeromagnetic characteristics.

Late-phase deposits were emplaced during a short interval (1.46–1.14 Ma) of the Matuyama magnetic chron but potentially encompass two reversed subchrons (fig. C5). No paleomagnetic data exist for the three volcanic units composing these late-phase eruptions, but existing age data, stratigraphic relations, and aeromagnetic data support the following preliminary interpretations: (1) The oldest eruptive center (unit Qba, fig. C2) produces a moderately strong negative polarity signature consistent with the 1.46 Ma $^{40}Ar/^{39}Ar$ age determination for this unit. (2) Unit Qd also produces a moderately strong negative polarity signature consistent with the 1.31 Ma $^{40}Ar/^{39}Ar$ age determination for this eruptive center. (3) Cochiti Cone (unit Qcc) produces predominantly strong negative aeromagnetic anomalies with the exception of strong positive anomalies observed near the base of the volcano on the west, southwest, and southeast shoulders (pl. 5). The $^{40}Ar/^{39}Ar$ age determination of 1.14±13 Ma for this center encompasses potentially two normal subchrons within the Matuyama,


Pleistocene
Pliocene
Late Phase
Middle Phase
Early Phase
Qec
Qcc
Qbt
Qd
Qbo
QTba
Ta
Tb4?
Tb3?
Tth
Tcmu?
Tb1
Tcp
Ttd
To
Tbr
Tae
Tcm
Tto
Tbu
Tbb
Tb
Tbt
Tb2
Tah
Tdt
Tat
Tcc
Tm
Tbj
Tbb
Tbs
Inferred or determined normal magnetic polarity
Inferred or determined reversed magnetic polarity

Figure C7 (facing page). Correlation of map units interpreted on the basis of known stratigraphic relations, $^{40}Ar/^{39}Ar$ geochronology, aeromagnetic data, and paleomagnetic determinations. Eruptive phases of the Cerros del Rio volcanic field indicated by brackets on right side of figure. Map unit symbols: QTba, basalt of Cochiti; Qbo, Otowi Member of Bandelier Tuff; Qbt, Tshirege Member of Bandelier Tuff; Qcc, basaltic andesite of Cochiti Cone; Qd, dacite of White Rock Canyon; Qec, El Cajete tephra; Ta, late andesite of Caja del Rio; Tae, andesite of Arroyo Eighteen; Tah, andesite of Hill 6385; Tat, andesite of Tetilla Peak; Tb_1, basalt of Hill 7071; Tb_2, basaltic andesite of Petroglyph Canyon; Tb_3, lower flow unit of Bajada Mesa; Tb_4, upper flow unit of Bajada Mesa; Tb, basalt of White Rock Canyon; Tbb, basalt of La Bajada; Tbj, basalt of Mesita de Juana Lopez; Tbr, basalt of Caja del Rio; Tbs, basalt of Tsinat Mesa; Tbt, basalt of Tetilla Hole; Tbu, basalt of Canada Ancha; Tcc, andesite of Cerro Colorado; Tcm, basaltic andesite of Cerro Micho; Tcmu, late andesite of Cerro Micho; Tcp, andesite of Cerro Portrillo; Tdt, dacite of Tetilla Peak; Tm, basaltic andesite of Cerro Montoso; To, andesite of Ortiz Mountain; Ttd, basaltic andesite of Tank 31; Tth, andesite of Twin Hills; Tto, basalt of Thirty One Draw.

both younger and older than the preferred age of 1.14 Ma. A reasonable interpretation is that early lavas of Cochiti Cone erupted during the short normal subchron of the Matuyama between 1.19 Ma and 1.21 Ma and that the main eruptive phase followed during a reversed magnetic subchron between 1.19 and 1.07 Ma. However, the relatively thin cover of Cochiti Cone lava flows may simply reflect the predominant aeromagnetic signature of underlying lava flows of normal magnetic affinity.

Structural Controls on Eruption

Most structures defining the boundaries of the La Bajada constriction are largely buried beneath Pliocene volcanic cover of the Cerros del Rio volcanic field (chapter G, this volume). Possible rift-related, northwest-trending faults and aeromagnetic lineaments similar to those in the northeast part of the Santo Domingo Basin are also obscured by volcanic cover east of the La Bajada fault zone. However, the timing of basaltic volcanism, its feeder mechanisms, and vent locations can be used to infer potential structural control on magma emplacement, providing constraints on subsurface fault geometries.

Early-phase volcanism appears to have been broadly distributed across the volcanic highlands and surrounding plateau that overlaps basin-fill deposits of the northeastern Santo Domingo and southern Española Basins. Vent locations at Mesita de Juana (unit Tbj), Tetilla Peak (unit Tat), Cerro Colorado (unit Tcc), and Cerro Montoso (unit Tm) exhibit a broad north-trending alignment (fig. C2). It is likely that these aligned large vents formed in response to broad, regional, east-west directed extension that was roughly perpendicular to the strikes of the younger La Bajada and Cochiti Cone faults farther west in the Cerros del Rio field.

Structural control on eruption mechanisms during the middle-phase eruptive episode is generally more difficult to discern, because lavas erupted from small systems with locally migrating vent areas characteristic of fissure-controlled basaltic eruptions. Numerous overlapping vents and local stratigraphic complexities obscure what was likely vent alignments based on evidence for comagmatic extensional faulting. Alignments of remnant cinder cones on La Bajada Mesa (pl. 1) (units Ta, Tbr; fig. C2) have northeast trends that broadly parallel locally exposed feeder dikes for these systems. These northeast trends are similar to the trend of a nearby geophysically inferred fault or fault zone buried beneath the Cerros del Rio volcanic field (pl. 2) that may form a structural boundary of the La Bajada constriction (chapters F and G, this volume). Thus, it is possible that the vent alignments are controlled by buried, preexisting faults.

Westward migration of active faulting (chapter E, this volume) after eruption of early- and middle-phase lavas is documented along the prominent escarpment of the La Bajada fault zone and in subtle surface expressions of faulting along the Cochiti Cone fault (CCF, fig. C2) and northern extensions of this system that form offset terraces in lava flows east of the Rio Grande in the northernmost part of the map area (pl. 2, fig. C2). These down-to-the-west normal faults, in conjunction with numerous subsidiary faults of similar orientation but lesser displacement, are at least partly responsible for maintaining the substantial topographic relief of the Cerros del Rio volcanic field east of the Rio Grande relative to middle-phase stratigraphic counterparts to the west.

Late-phase volcanism is restricted to centers west of the Cochiti Cone fault. Two primary vent areas for Cochiti Cone (unit Qcc, fig. C2), which are in the hanging-wall block of this fault and whose alignment parallels the presumed trace of the fault, were likely controlled by it. Units produced by all three late eruptive centers (units Qcc, Qd, QTba) are confined to a narrow corridor structurally bordered by the youngest faulting events (chapter E, this volume). Smith, Bailey, and Ross (1970) have depicted several vent areas for Cochiti Cone, including isolated vents west of the easternmost La Bajada fault strand in the area of the Solar T windmill of Cochiti Pueblo (plate 2 and marked Solar TW on fig. G1). Recent mapping suggests that Cochiti Cone eruptions may be in part coeval with displacement along the northernmost part of the La Bajada fault zone and in places postdate major offset. Lava flows from Cochiti Cone vent areas east of the northern La Bajada escarpment cascaded westward over the eastern La Bajada fault scarp to form much of the lower plateau surface containing the solar windmill. This history accounts for the lack of near-vent deposits on the lower surface and negates the requirement of separate vent areas for Cochiti Cone deposits west of the eastern La Bajada fault strand.

Summary

1. Stratigraphic and geochronologic data for Cenozoic volcanic rocks of the La Bajada constriction region are used to constrain the spatial and temporal evolution of rift-related faulting and basin formation in the zone of structural overlap between the Santo Domingo and Espanola Basins of the Rio Grande rift.

2. Pliocene volcanic deposits of the Cerros del Rio largely obscure pre-rift and early rift structures that control local deposition of basin-fill sediments in the La Bajada constriction area. Structural control of volcanism is also obscured by limited exposure and is complicated by a history of many phases of eruption from many centers of variable age, composition, and volume. However, Pliocene volcanism of the Cerros del Rio can be divided into early, middle, and late eruptive phases that reflect generally decreasing areal extent and eruptive volume with time.

3. Vent areas were predominantly single-vent, low-angle, shield volcanoes, multivent cinder-cone complexes, orcinder-cone clusters related to structurally controlled fissure eruptions. A general northeast alignment of middle-phase vent areas may reflect structural control of subsurface plumbing systems. All volcanoes were dike fed; dikes are variably oriented, but preliminary evidence suggests that larger vent complexes trend predominantly northeast.

4. Vents and vent alignments of late-phase eruptive centers step to the west as compared with early- and middle-phase eruptive centers. Vent locations appear to migrate in response to westward migration of active major down-to-west normal faults. The topographic high which Pleistocene Bandelier Tuff abuts is related to constructive topography associated with Cerros del Rio vent areas in addition to structural relief related to throw along the La Bajada fault zone, Cochiti Cone fault, and subsidiary faults.

References Cited

Aubele, J.C., 1978, Geology of the Cerros del Rio volcanic field, Santa Fe, Sandoval, and Los Alamos Counties, New Mexico: Albuquerque, University of New Mexico, M.S. thesis, 136 p.

Aubele, J.C., 1979, The Cerros del Rio volcanic field: New Mexico Geological Society 30th field conference, Santa Fe Country, Guidebook, p. 243–252.

Bachman, G.O., and Mehnert, H.H., 1978, New K-Ar dates and the late Pliocene to Holocene geomorphic history of the central Rio Grande region, New Mexico: Geological Society of America Bulletin, v. 89, no. 2, p. 283–292.

Bailey, R.A., Smith, R.L., and Ross, C.S., 1969, Stratigraphic nomenclature of volcanic rocks in the Jemez Mountains, New Mexico: U.S. Geological Survey Bulletin 1274–P, p. 1–19.

Baldridge, W.S., 1979a, Petrology and petrogenesis of Plio-Pleistocene basaltic rocks from the central Rio Grande rift, New Mexico, and their relation to rift structure, *in* Riecker, R.E., ed., Rio Grande rift—Tectonics and magmatism: American Geophysical Union, Washington, D.C., p. 323–353.

Baldridge, W.S., 1979b, Mafic and ultramafic inclusion suites from the Rio Grande rift (New Mexico) and their bearing on the composition and thermal state of the lithosphere: Journal of Volcanology and Geothermal Research, v. 6, p. 319–351.

Baldridge, W.S., Damon, P.E., Shafiqullah, M., and Bridwell, R.J., 1980, Evolution of the central Rio Grande rift, New Mexico—New potassium-argon ages: Earth and Planetary Science Letters, v. 51, p. 309–321.

Baldridge, W.S., Olsen, K.H., and Callender, J.F., 1984, Rio Grande rift, problems and perspectives: New Mexico Geological Society 35th field conference, Rio Grande Rift—Northern New Mexico, Guidebook, p. 1–12.

Bartolino, J.R., and Cole, J.C., 2002, Ground-water resources of the Middle Rio Grande Basin, New Mexico: U.S. Geological Survey Circular 1222, 132 p.

Bryan, Kirk, 1938, Geology and ground-water conditions of the Rio Grande depression in Colorado and New Mexico: National Resource Commission, Washington, Regional Planning, pt. 6, Rio Grande joint investigations in the upper Rio Grande Basin, v. 1, pt. 2, sec. 1, p. 197–225.

Dethier, D.P., 1997, Geology of the White Rock quadrangle, Los Alamos and Santa Fe Counties, New Mexico: New Mexico Bureau of Mines and Mineral Resources Geologic Map GM–73, scale 1:24,000.

Disbrow, A.E., and Stoll, W.C., 1957, Geology of the Cerrillos area, Santa Fe County, New Mexico: New Mexico Bureau of Mines and Mineral Resources Bulletin 48, 73 p.

Dungan, M.A., Thompson, R.A., Stormer, J.S., and O'Neill, J.M., 1989, Rio Grande rift volcanism—Northeastern Jemez zone, New Mexico: New Mexico Bureau of Mines and Mineral Resources Memoir 46, p. 435–486.

Dunker, K.E., Wolfe, J.A., Harmon, R.S., Leat, P.T., Dickin, A.P., and Thompson, R.N., 1991, Diverse mantle and crustal components in lavas of the NW Cerros del Rio volcanic field, New Mexico: Contributions to Mineralogy and Petrology, v. 108, p. 331–345.

Fisher, R.A., 1953, Dispersion on a sphere: Proceedings of the Royal Society [London], Series A217, v. 295–305.

Gardner, J.N., Goff, Fraser, Garcia, S., and Hagan, R.C., 1986, Stratigraphic relations and lithologic variations in the Jemez volcanic field, New Mexico: Journal of Geophysical Research, v. 91, p. 1763–1778.

Goff, Fraser, Gardner, Jamie, and Valentine, Greg, 1990, Geologic map of the St. Peters Dome area, Jemez Mountains, New Mexico: New Mexico Bureau of Mines and Mineral Resources Geologic Map 69, scale 1:24,000.

Grauch, V.J.S., and Bankey, Viki, 2003, Aeromagnetic interpretations for understanding the hydrogeologic framework of the southern Española Basin, New Mexico: U.S. Geological Survey Open-File Report 03–124, available from http://pubs.usgs.gov/of/2003/ofr–03–124/.

Griggs, R.L., 1964, Geology and groundwater resources of the Los Alamos area, New Mexico: U.S. Geological Survey Water-Supply Paper 1753, 107 p.

Halls, H.C., 1976, A least-squares method to find remanence directions from converging remagnetization circles: Geophysical Journal of the Royal Astronomical Society, v. 45, p. 297–304.

Justet, Leigh, 1999, The geochronology and geochemistry of the Bearhead Rhyolite, Jemez volcanic field, New Mexico: Las Vegas, University of Nevada, M.S. thesis, 152 p.

Kelley, V.C., and Kudo, A.M., 1978, Volcanoes and related basalts of Albuquerque Basin, New Mexico: New Mexico Bureau of Mines and Mineral Resources Circular 156, 30 p.

Kirschvink, J.L., 1980, The least-squares line and plane and the analysis of paleomagnetic data: Geophysical Journal of the Royal Astronomical Society, v. 62, p. 699–718.

Lavine, Alex, Smith, G.A., and Goff, Fraser, 1996, Volcaniclastic rocks of the Keres Group—Insights into mid-Miocene volcanism and sedimentation in the southeastern Jemez Mountains: New Mexico Geological Society 47th field conference, Jemez Mountains Region, Guidebook, p. 211–218.

Le Bas, M.J., Le Maitre, R.W., Streckeisen, A., and Zanettin, B., 1986, A chemical classification of volcanic rocks based on the total alkali-silica diagram: Journal of Petrology, v. 27, p. 745–750.

Lipman, P.W., 1988, Evolution of silicic magma in the upper crust—The mid-Tertiary Latir volcanic field and its cogenetic granitic batholith, northern New Mexico, USA: Royal Society of Edinburgh—Earth Science, Transactions, 79, p. 265–288.

Lipman, P.W., and Mehnert, H.H., 1979, The Taos Plateau volcanic field, northern Rio Grande rift, New Mexico, *in* Riecker, R.E., ed., Rio Grande rift—Tectonics and magmatism: Washington, D.C., American Geophysical Union, p. 289–309.

Luedke, R.G., and Smith, R.L., 1978, Map showing the distribution, composition, and age of the late Cenozoic volcanic centers in Arizona and New Mexico: U.S. Geological Survey Miscellaneous Investigations Series Map I–1091A, scale 1:1,000,000.

Mayo, E.B., 1958, Lineament tectonics and some ore districts of the southwest: Mining Engineering, v. 10, p. 1169–1175.

McIntosh, W.C., and Quade, Jay, 1995, $^{40}Ar/^{39}Ar$ geochronology of tephra layers in the Santa Fe Group, Española Basin, New Mexico: New Mexico Geological Society 46th field conference, Santa Fe Region, Guidebook, p. 279–287.

McMillan, N.J., 1998, Temporal and spatial magmatic evolution of the Rio Grande rift: New Mexico Geological Society 49th field conference, Las Cruces Country II, Guidebook, p. 107–116.

Miggins, D.P., Thompson, R.A., Pillmore, C.L., Snee, L.W., and Stern, C.R., 2002, Extension and uplift of the northern Rio Grande rift—Evidence from $^{40}Ar/^{39}Ar$ geochronology from the Sangre de Cristo Mountains, south-central Colorado and northern New Mexico, *in* Menzies, M.A., Klemperer, S.L., Ebinger, C.J., and Baker, J., eds., Volcanic rifted margins: Geological Society of America Special Paper 362, p. 47–74.

Minor, S.A., and Hudson, M.R., 2006, Regional survey of structural properties and cementation patterns of fault zones in the northern part of the Albuquerque Basin, New Mexico—Implications for ground-water flow: U.S. Geological Survey Professional Paper 1719, 28 p.

Onstott, T.C., 1980, Application of the Bingham distribution function in paleomagnetism studies: Journal of Geophysical Research, v. 85, p. 1500–1510.

Personius, S.F., 2002, Geologic map of the Santa Ana Pueblo quadrangle, Sandoval County, New Mexico: U.S. Geological Survey Miscellaneous Field Studies Map MF–2405, scale 1:24000.

Reneau, S.L., Gardner, J.N., and Forman, S.L., 1996, New evidence for the age of the youngest eruption in the Valles caldera, New Mexico: Geology, v. 24, p. 7–10.

Reneau, S.L., McDonald, E.V., Gardner, J.N., Kolbe, T.R., Carney, J.S., Watt, P.M., and Longmire, P.A., 1996, Erosion and deposition on the Pajarito Plateau, New Mexico, and implications for geomorphic responses to late Quaternary climatic change: New Mexico Geological Society 47th field conference, Jemez Mountains Region, Guidebook, p. 391–397.

Sauer, R.R.,1999, Petrochemistry and geochronology of plutons relative to tectonics in the San Pedro–Ortiz porphyry belt, New Mexico: Boulder, University of Colorado, M.S. thesis, 115 p.

Sawyer, D.A., Shroba, R.R., Minor, S.A., and Thompson, R.A., 2002, Geologic map of the Tetilla Peak quadrangle, Santa Fe and Sandoval Counties, New Mexico: U.S. Geological Survey Miscellaneous Field Studies Map MF–2352, scale 1:24,000.

Smith, G.A., and Kuhle, A.J., 1998a, Geology of the Santo Domingo Pueblo quadrangle, Sandoval County, New Mexico: New Mexico Bureau of Mines and Mineral Resources Open-file Geologic Map OF–GM 15, scale 1:24,000.

Smith, G.A., and Kuhle, A.J., 1998b, Geology of the Santo Domingo SW quadrangle, Sandoval County, New Mexico: New Mexico Bureau of Mines and Mineral Resources Open-file Geologic Map OF–GM 26, scale 1:24,000.

Smith, R.L., and Bailey, R.A., 1966, The Bandelier Tuff—A study of ash-flow eruption cycles from zoned magma chambers: Bulletin of Volcanology, v. 29, p. 83–104.

Smith, R.L., and Bailey, R.A., 1968, Resurgent cauldrons, *in* Coats, R.R., Hay, R.L., and Anderson, C.A., eds., Studies in volcanology: Geological Society of America Memoir 116, p. 613–662.

Smith, R.L., Bailey, R.A., and Ross, C.S., 1970, Geologic map of the Jemez Mountains, New Mexico: U.S. Geological Survey Miscellaneous Investigations Map I–571, scale 1:125,000.

Spiegel, Zane, and Baldwin, Brewster, 1963, Geology and water resources of the Santa Fe area, New Mexico: U.S. Geological Survey Water-Supply Paper 1525, 258 pp.

Stearns, C.E., 1953, Tertiary geology of the Galisteo-Tonque area, New Mexico: Geological Society of America Bulletin, v. 64, p. 459–508.

Sun, Ming-shan, and Baldwin, Brewster, 1958, Volcanic rocks of the Cienega area, Santa Fe County, New Mexico: New Mexico Bureau of Mines and Mineral Resources Bulletin 54, 80 p.

Thompson, R.A., Dungan, M.A., and Lipman, P.W., 1986, Multiple differentiation processes in early rift calc-alkaline volcanics, northern Rio Grande rift, New Mexico: Journal of Geophysical Research, v. 91, p. 6046–6058.

Thompson, R.A., Johnson, C.M., and Mehnert, H.H., 1991, Oligocene basaltic volcanism of the northern Rio Grande rift–San Luis Hills, Colorado: Journal of Geophysical Research, v. 96, p. 13,577–13,592.

WoldeGabriel, Giday, Laughlin, A.W., Dethier, D.P., and Heizler, M., 1996, Temporal and geochemical trends of lavas in White Rock Canyon and the Pajarito Plateau, Jemez volcanic field, New Mexico, USA: New Mexico Geological Society 47th field conference, Jemez Mountains Region, Guidebook, p. 251–261.

WoldeGabriel, Giday, Warren, R.G., Broxton, D.E., Vaniman, D.T., Heizler, M.T., Kluk, E.C., and Peters, L., 2001, Episodic volcanism, petrology, and lithostratigraphy of the Pajarito Plateau and adjacent areas of the Española Basin and the Jemez Mountains: New Mexico Museum of Natural History and Science Bulletin, vol. 18, p. 97–129.

Wolf, J.A., Gardner, J.N., and Reneau, S.L., 1996, Field characteristics of the El Cajete pumice deposit and associated southwestern moat rhyolites of the Valles caldera: New Mexico Geological Society 47th field conference, Jemez Mountains Region, Guidebook, p. 311–316.

Wolf, J.A., Heikoop, C.E., and Ellisor, R., 2000, Hybrid origin of Rio Grande rift hawaiites: Geology, v. 28, no. 3, p. 203–206.

Zimmerman, C., and Kudo, A.M., 1979, Geology and petrology of Tetilla Peak: New Mexico Geological Society 30th field conference, Santa Fe Country, Guidebook, p. 253–256.

Published in the Central Region, Denver, Colo.
Manuscript approved for publication February 10, 2006
Graphics by authors
Photocomposition by Mari L. Kauffmann (Contractor, ATA Services)
Edited by Mary-Margaret Coates (Contractor, ATA Services)